



A Parametric Study to Improve the Heat Transfer of Solar Air Heater Through CFD Analysis

Mayank Sharma¹, Emarti Kumari², P.M. Meena³

^{1,2,3}Department of Mechanical Engineering, MBM University, Jodhpur, India

²emarti.me@mbm.ac.in

How to cite this paper: M. Sharma, E. Kumari and P. M. Meena, "A parametric study to improve the heat transfer of solar air heater through CFD analysis," *Journal of Mechanical and Construction Engineering (JMCE)*, Vol. 02, Iss. 02, S. No. 004, pp. 1–17, 2022.

<https://doi.org/10.54060/jmce.v2i2.22>

Received: 30/09/2022

Accepted: 31/10/2022

Published: 25/11/2022

Copyright © 2022 The Author(s).

This work is licensed under the Creative Commons Attribution International License (CC BY 4.0).

<http://creativecommons.org/licenses/by/4.0/>



Open Access

Abstract

In this article, we optimize the performance of a solar air heater (SAH) using two designs and computational fluid dynamics (CFD) analysis in this article. With the help of ANSYS fluent, two designs are considered to investigate the effect of different rib heights ($e = 1, 1.2, 1.4, 1.6, \text{ and } 1.8$) and duct depths ($h = 16, 18, 20, 22, \text{ and } 24$). The effects of different parameters such as velocity, temperature, turbulence kinetic energy, and turbulence energy are compared to optimize the performance of designs 2 and 3. It is noticed that except temperature, all other parameters are on the lower side for design 2 as compared to design 3, due to improper air mixing in design 2. The authors presented the optimized design 3 with rib height $e = 1.8$ and depth of duct $h = 16$ after consideration of all the parameters (temperature, velocity, turbulence kinetic energy, and turbulence intensity) at various rib heights and depths of duct. These numerical results will serve as a benchmark for future research to improve the efficacy of solar air heaters.

Keywords

Solar air heaters, CFD, Rib-height, Depth of duct, Simulation

1. Introduction

The energy obtained by collecting the Sun's heat and light is known as solar energy. Solar energy is the energy that comes from the Sun. This rich resource may now be used in a variety of ways thanks to technological advancements [1]. Because it does not



emit greenhouse gases, it is considered a green technology. Solar energy is plentiful and has long been used as both a source of power and a source of heat[2]. Solar technology may be divided into two categories: Active and Passive.

To harness the energy, active solar approaches such as photovoltaic systems, concentrated solar power, and solar water heating are used. Active solar is used directly in activities like drying clothes and heating the air. Passive solar heating orient a structure to the Sun, selecting materials with favourable thermal mass or light-dispersing characteristics, and creating areas that naturally circulate air are all examples of passive solar methods [3]. Recently, investigated the static and dynamic characteristics of curved panels by [16-19] employing finite element formulation based on first order shear deformation theory.

1.1. Solar Heating

Solar heating is a renewable energy system that absorbs energy from the sun in the form of heat rather than using it to generate electricity, like solar photovoltaic does [4]. Solar heating systems can be utilised in residential, commercial, or industrial buildings to offer space and water heating[5]. Solar air heating technology uses only clean, renewable and free energy and can help reduce rising conventional energy costs. A solar air heating system absorbs heat from direct sunlight to heat the air; this heated air can circulate through buildings to provide heat [6-7].

1.2 Mechanism of Heating

Elementarily heating composes of two basic and simultaneous processes: (a) mass is transferred as a liquid or vapor within the solid and as a Vapour from the surface (b) heat is moved to evaporate the liquid. The aspects leading the rates of these processes conclude the heating rate[8 -9].

The structure of the solid concludes the mechanism for which internal liquid flow may occur and these mechanisms can be stated as[10].

1. Capillary flow in porous and granular solids
2. Diffusion in uniform and uninterrupted solids
3. Flow due to a vaporization and condensation chain
4. Flow due to pressure gradients and contraction
5. Flow of liquid due to gravity

2. Methodology

The scope of this work is multiple; the study covers the study of the parameters, a design study taking into account the technological considerations due to the CFD analysis of the solar air heater, at the level of the system, the study approach is placed in several studies of parameters that are important for understanding solar work heaters. At the level of components, a combination of study of two new different designs by varying different designs and lead a study based on the comparison and, together with it, an experimental validation is carried out [11-12].

Table 1. Different parameters and their ranges

Parameters	Range
Entrance length of duct, L1	245 mm
Test length of duct, L2	300 mm
Exit length of duct, L3	120 mm
Width of duct, W	100 mm

Depth of duct, H	16, 18, 20, 22, 24 mm
Rib height, e	1.0, 1.2, 1.4, 1.6, 1.8 mm
Rib Pitch, P	10
Reynolds number, Re	15000
Prandtl number, Pr	0.7441
Heat Flux, I	1000 W/m ²

2.1 Hydraulic diameter of duct

The hydraulic diameter, D_h , is a commonly used term when handling flow in non-circular tubes and channels. Various parameters and the range of these parameters is given in **Table 1**. The hydraulic diameter transforms non-circular ducts into pipes of equivalent diameter. Using this term, one can calculate many things in the same way as for a round tube. In this equation A is the cross-sectional area, and P is the wetted perimeter of the cross-section.

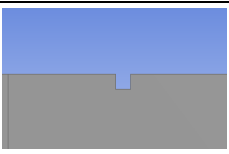


$$D_h = \frac{4 \times W \times H}{2(W + H)}$$

$$D_h = \frac{4 \times 100 \times 20}{2(100 + 20)} = 33.33 \text{ mm}$$

Here W and H are width and depth of duct; respectively.

2.2 Case design

Table 2. Various designs to enhance the heat transfer of solar air heater

Design	e (mm)	D (mm)	Image
Design 1	1.4	33.33	
Design 2	1.0	27.59	
	1.2	30.51	
	1.4	33.33	
	1.6	36.07	
	1.8	38.71	
Design 3	1.0	27.59	
	1.2	30.51	
	1.4	33.33	
	1.6	36.07	
	1.8	38.71	

The design of the ribs in the absorber plate will be varied in the CFD model for different values of $e = 1.0, 1.2, 1.4, 1.6$ and 1.8 . The various values obtained for rib-height e are presented in **Table 2**. Three designs are given in **Table 2** with rectangular cross-section, U -shape cross-section and V -shape cross-section in Design 1, Design 2 and Design 3; respectively.

2.3 Material Property

The material properties have a distinct role in CFD modeling as they will be used to simulate the flow material. The properties for Air and aluminum are given in the **Table 3**.

Table 3. Properties of Air and Aluminum considered for CFD analysis.

Properties	Air	Aluminium
Density, ρ (kg/m ³)	1.225	2719
Specific heat, C_p (kJ/kg-K)	1006.43	871
Viscosity, μ (N-s/m ²)	1.7894e-05	--
Thermal conductivity, K (W/m-K)	0.0242	202.4

3. Design in Ansys Modular

Figure1 shows the details about the design of the absorber plate along with the ribs incorporated in them as per the design parameters discussed above. The design of absorber plate will be used in CFD model for analysis.

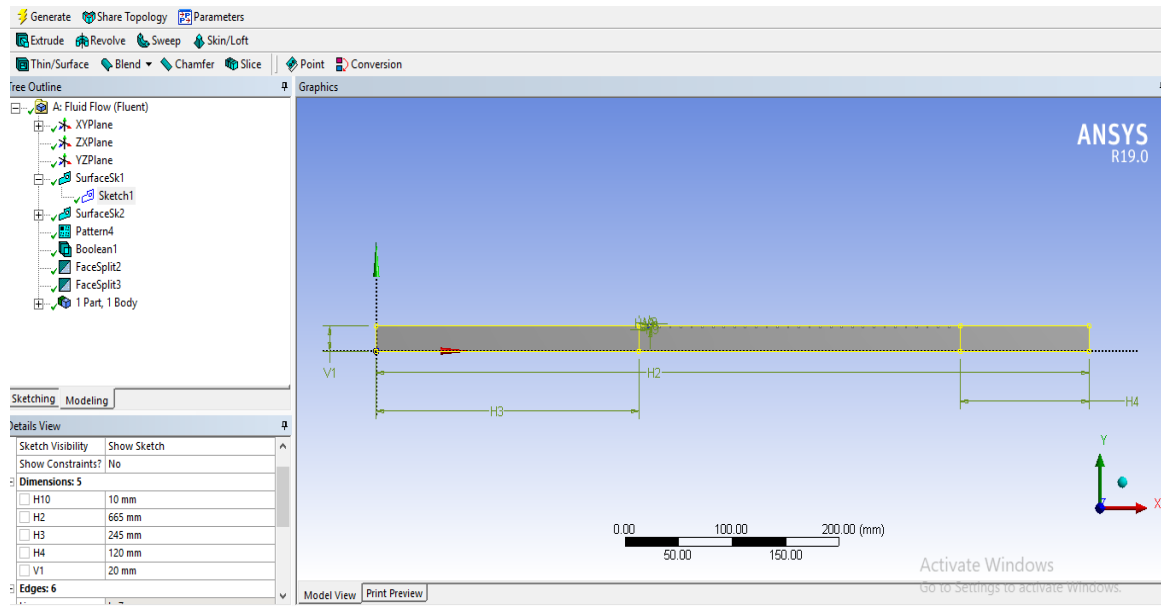


Figure 1. Design in ANSYS Design modular

3.1. Name Selection

The different sections of the absorber plate are identified as given nomenclature in **Figure2**; A – Inlet, B – outlet, C – Absorber plate, D – Inlet Top, E – Inlet Bottom, F – Outlet Top, G – Outlet Bottom, H – Absorber plate bottom. **Figure 2** will be helpful in identification and understanding the functions of absorber plate.

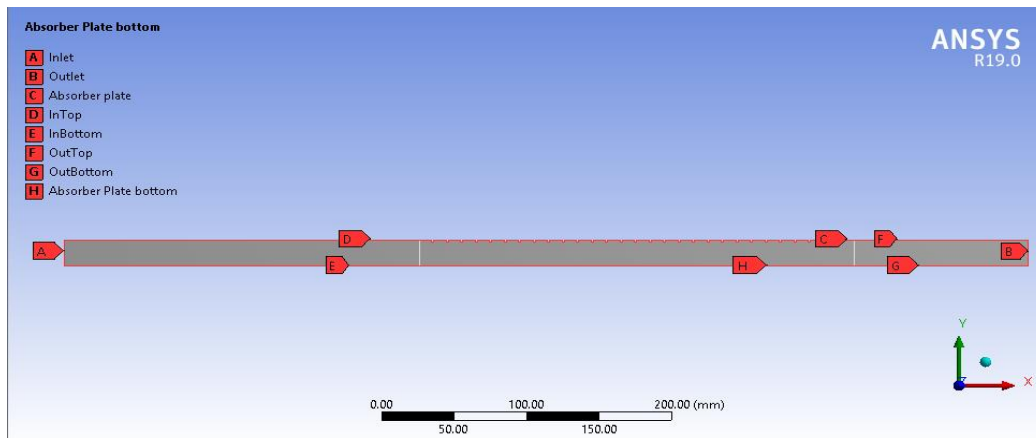
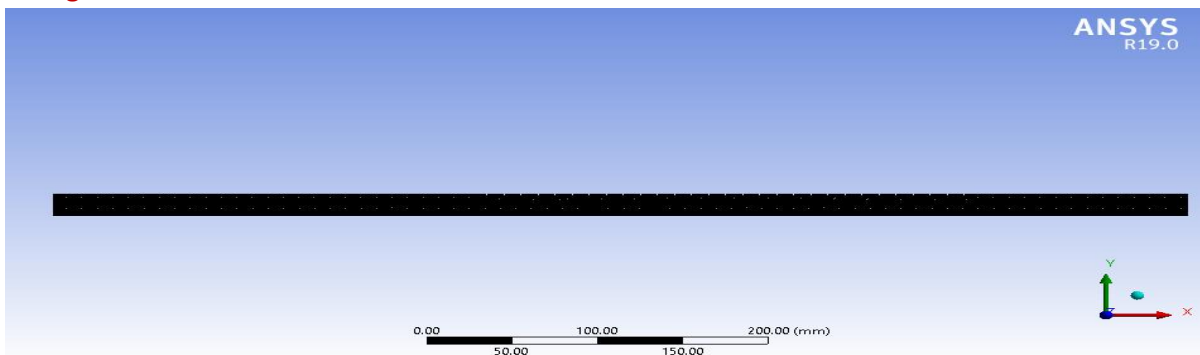
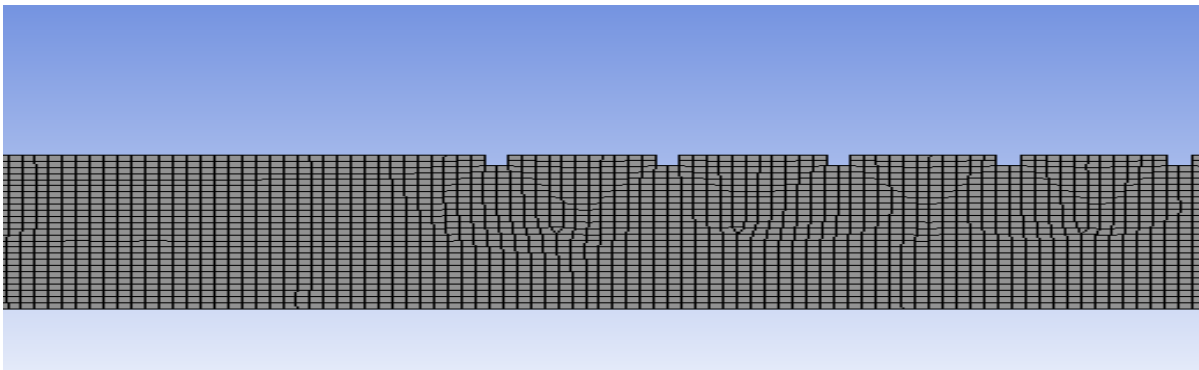


Figure 2. Different selections of absorber plate

3.2. Meshing



(a) Quadrilateral Meshing of solar air heater



(b) Zoomed view of Quadrilateral Meshing

Figure 3. Meshing of Solar Air Heater

For meshing Quadrilateral element is used to mesh the solar air heater as presented in **Figure 3(a)**. To mesh the present model of solar air heater 20770 elements and 21678 nodes are created and zoomed view of it is presented in **Figure 3 (b)**.

3.3. Boundary Condition

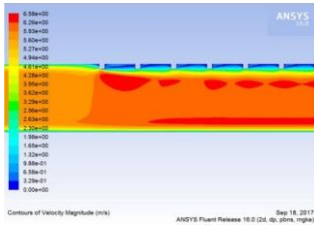
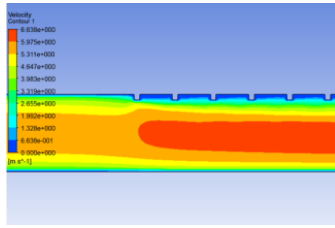
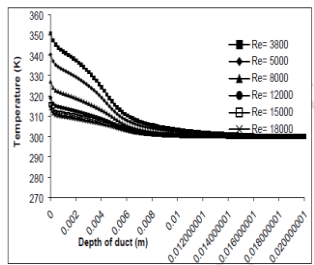
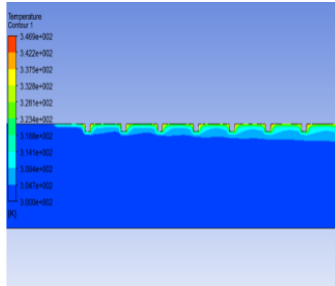
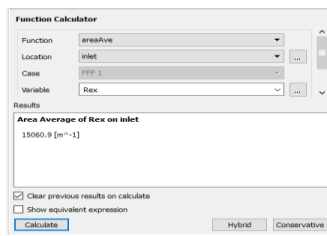
The left edge is assumed as inlet and right edge as outlet. The top edges of the duct are named as in top, absorber plate and out top. Bottom edge may be specified as insulation to avoid heat loss by conduction and convection. A velocity condition might be given at inlet and atmospheric pressure outlet at exit boundary condition. The air enters into the entrance section at 300 K when no-slip conditions considered over duct walls. A constant heat flux (1000 W/m²) is used on the absorber plate.

4. Results and discussions

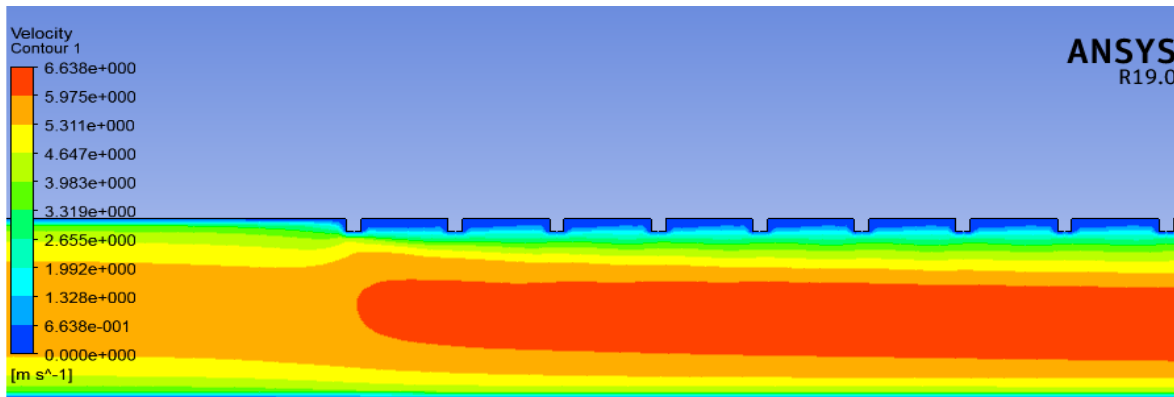
4.1 Validation of Result

Firstly, a validation study was performed to check the accuracy of present numerical results with available published results. Design 1 is considered here for validation study and compared the present numerical results with computational fluid dynamic results [13 – 15] and computational fluid dynamic results are presented in **Table 4**. Percentage of error is 0.87% and 1.21% with published result by [14] for maximum velocity and maximum temperature attained in solar air heater; respectively. Moreover, percentage of error is 0.4% with available result by Abn and Son [15] for case of Reynold’s number.

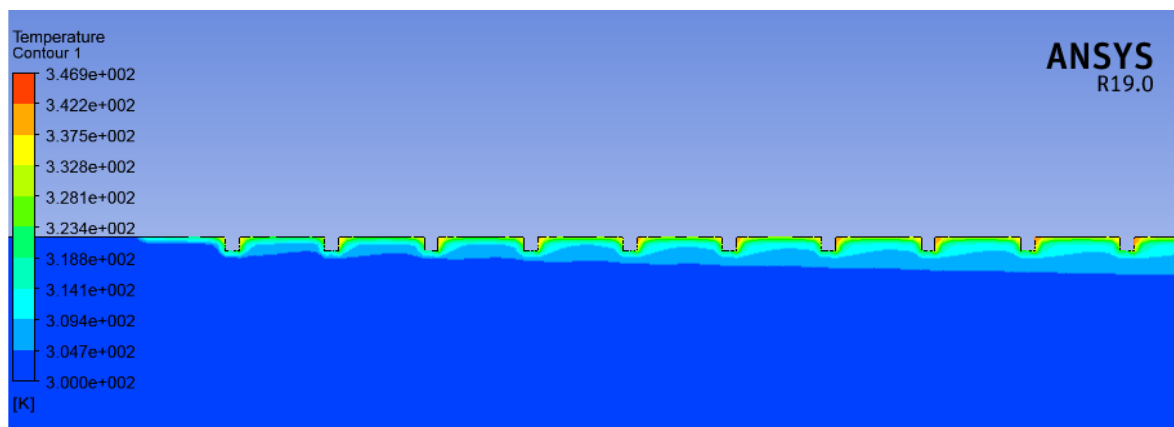
Table 4. Comparison of velocity, temperature and Reynold’s number with available published numerical results

Parameter	Base Paper	Present	Validation
Velocity			Maximum velocity attained in the present study is 6.638 m/s which is similar to 6.58 m/s of Abhay <i>et al.</i> [14].
Temperature			Maximum temperature attained in the present study is 346.2K which comparatively similar to 342K of Abhay <i>et al.</i> [14].
Reynold's number (Experimental result) [5]	15000		This paper evaluated Reynolds number of 15060.9 which is similar to that of 15000 attained by Abn and Son[15].

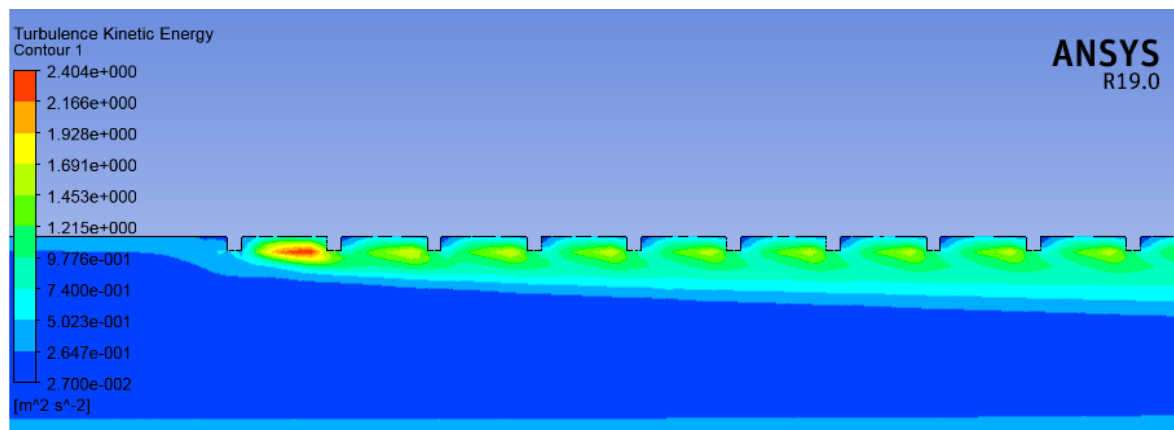
4.2 Result for Design 1 at $e = 1.4$



(a) Velocity Contour



(b) Temperature Contour



(c) Turbulence KE contour

Figure 4. Contour plots for Design 1 ($e = 1.4$)

The maximum velocity was found to be 6.638 (m/s) in the middle section of the absorber plate shown in orange shaded region. Near ribs and at bottom most area it is observed to be 0 (m/s) as shown by blue shaded regions.

The velocity is higher in the middle region of the absorber plate, the temperature doesn't increase at middle section of the plate, temperature will increase near the ribs; change in temperature will be seen (shown in yellow and red regions) up to 348.1K. Rest of the area in the absorber plate shown by blue shades has temperature near to the inlet air temperature ranging from 300K to 319K which means that high temperature is only obtained at the top of the plate and is not properly distributed throughout the duct.

The turbulence kinetic energy contour at $e=1.4$ Figure 4 shows that the turbulent kinetic energy is high at regions near to the ribs shown by yellow-green shades reaching up to $2.404 \text{ (m}^2/\text{s}^2\text{)}$ but we are not getting high value of turbulence intensity throughout the absorber plate therefore to solve this problem we need to change the design and also vary different parameters to increase the heat transfer of solar air heater.

4.3 Performance of Design 2 for various rib height and depth of duct

4.3.1 Result with change in rib height (e)

It is evident from the resultant values from **Figure 5** that the Velocity is increased from 6.628 to 6.685m/s by increasing the rib height $e = 1.0$ to 1.8 and corresponding value of temperature, turbulence and turbulence intensity for $e = 1.8$ are 346.1K, $2.371 \text{ m}^2/\text{s}^2$ and 1.256; respectively which means that higher side value of rib-height (e) is desirable for Design 2 that is presented in **Table 5**.

Table 5. Variation of parameters with respect to rib-height (e) and depth of duct (h) for **Design 2**.

		Velocity (m/s)	Temperature (K)	Turbulence Kinetic Energy (m^2/s^2)	Turbulence Intensity
Rib-height (e)	1.0	6.628	346.7	2.618	1.318
	1.2	6.577	343.3	2.366	1.243
	1.4	6.590	348.1	2.062	1.169
	1.6	6.696	352.4	2.136	1.191
	1.8	6.858	346.1	2.371	1.256
depth of duct (h)	16	6.686	347.3	2.312	1.237
	18	6.637	347.7	2.202	1.208
	20	6.590	348.1	2.062	1.169
	22	6.551	348.6	2.398	1.261
	24	6.515	349.1	2.146	1.194

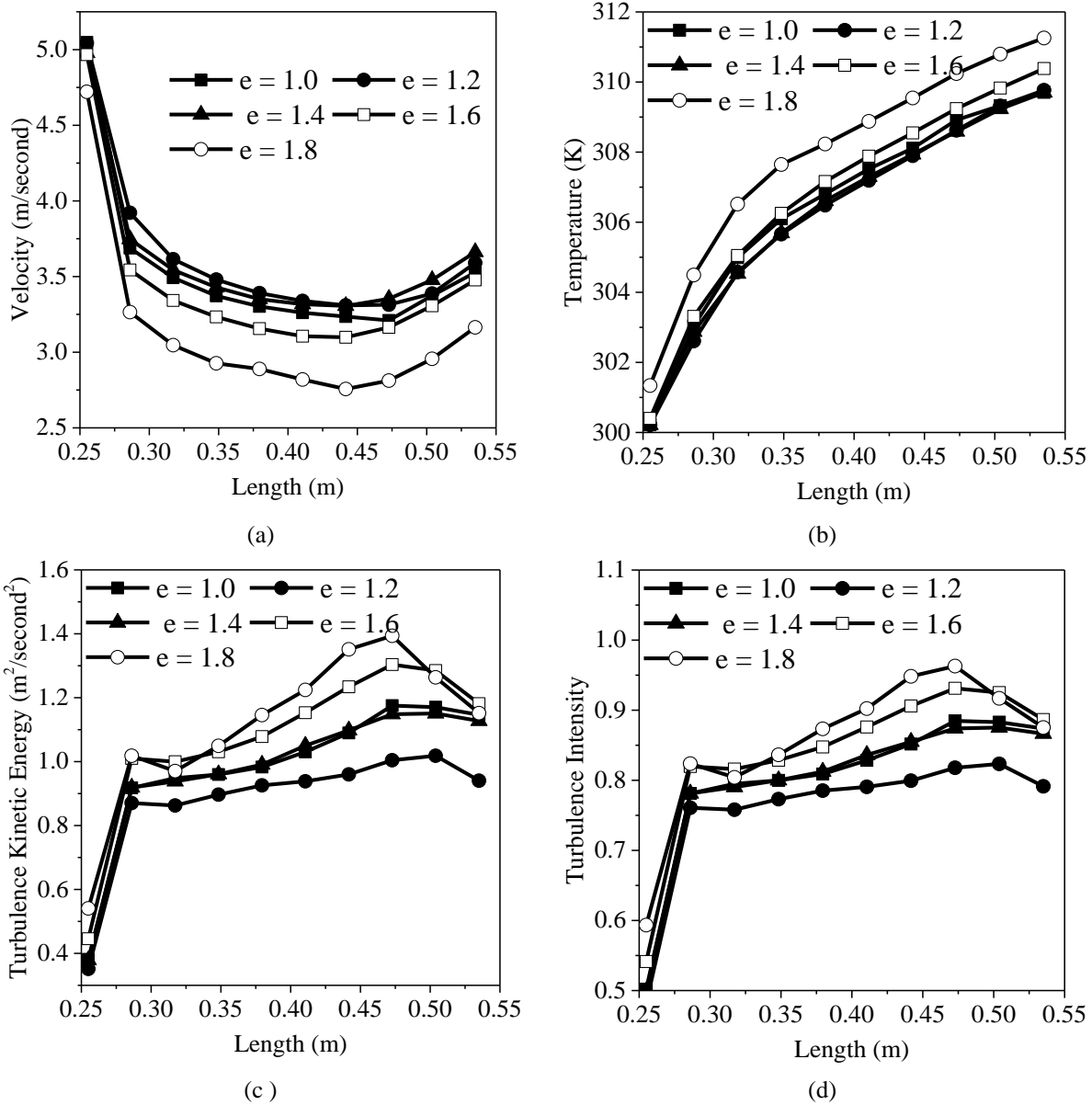


Figure 5. Comparison of different values of e for (a) velocity, (b) temperature, (c) turbulence KE and (d) turbulence intensity for Design 2

4.3.2 Result with change in depth of duct (h)

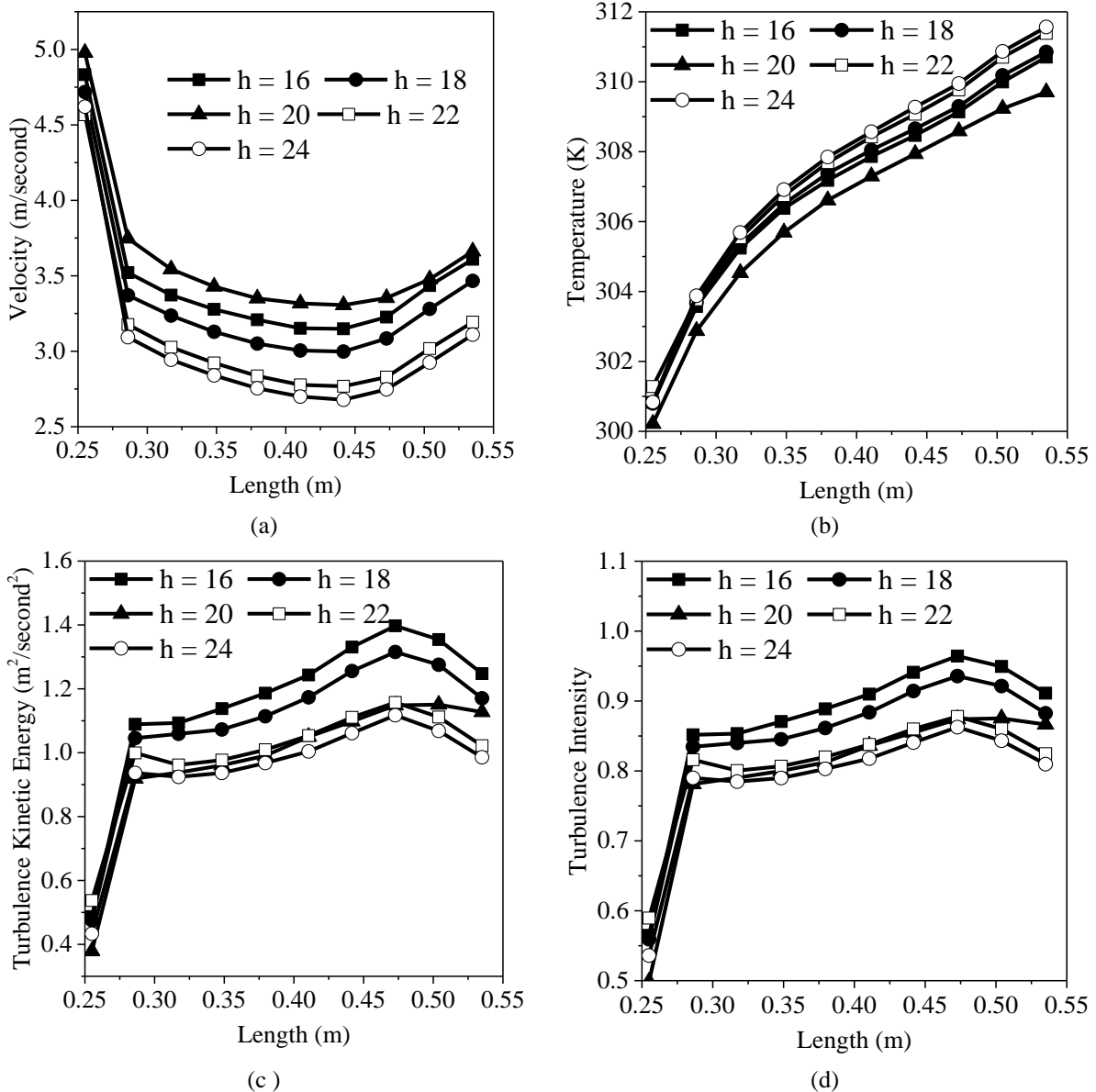


Figure 6. Comparison of different values of h for (a) velocity, (b) temperature, (c) turbulence KE and (d) turbulence intensity for Design 2.

The following results were obtained after changing the different value of (h) Depth of duct as shown in Figure 6. The depth of the duct (h) shows the reverse response with change in depth of duct from $h = 16, 18, 20, 22, 24$ as compare to height of rib. It is noticed that the velocity is decreased from 6.686 to 6.515 m/s on increasing the depth of duct, therefore $h=16$ shows best results having uniform distribution of temperature throughout and highest value of turbulence kinetic energy and intensity $2.618\text{m}^2/\text{s}^2$ and 1.237; respectively.

4.4 Design 3

4.4.1 Effect of rib height (e)

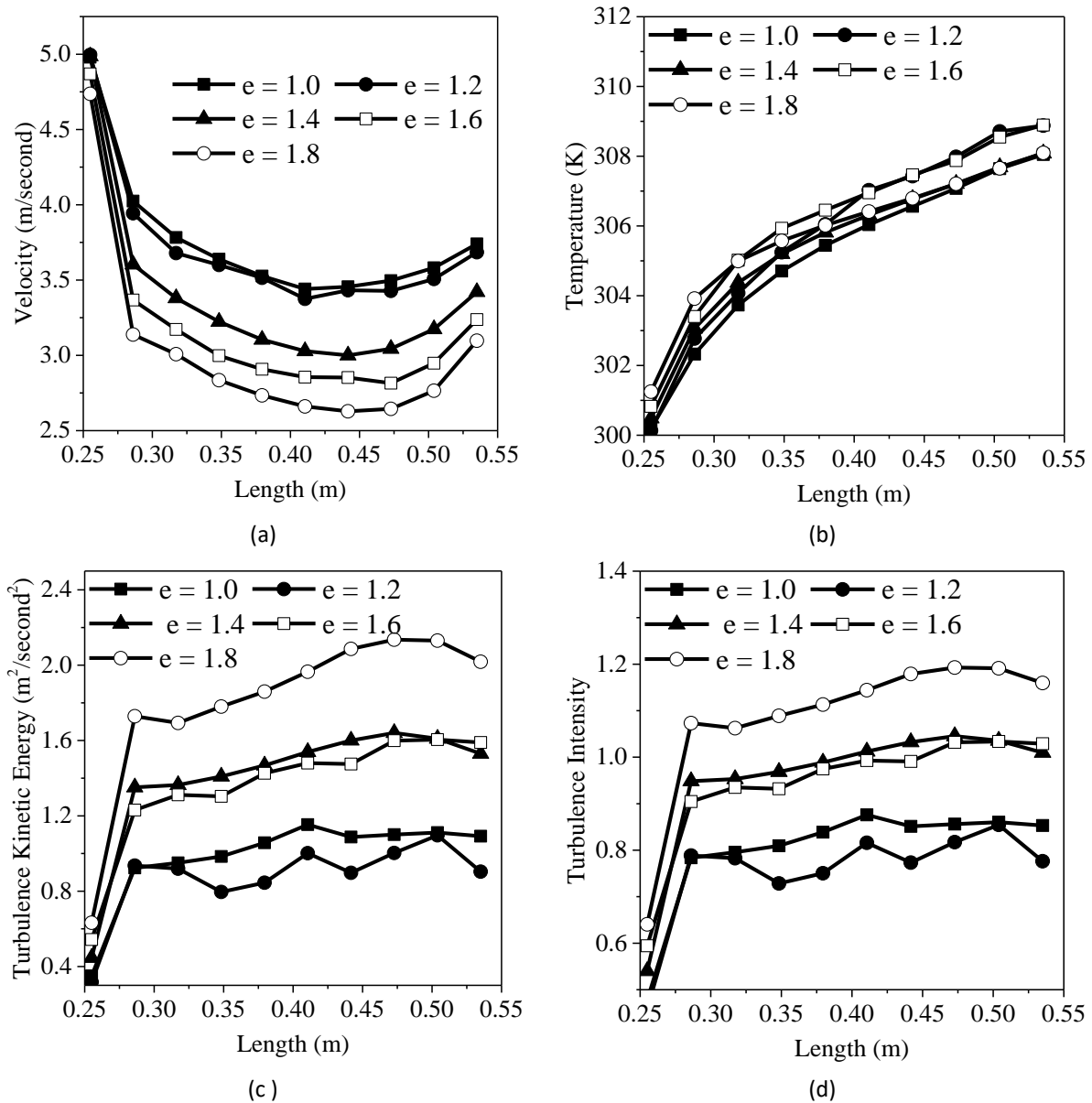


Figure 7. Comparison of different values of e for (a) velocity, (b) temperature, (c) turbulence KE and (d) turbulence intensity for **Design 3**.

Now, the effect of rib height is examined for design 3 and results are presented in **Figure 7**. It is observed that the above graphs that value of velocity keeps on increasing with respect to the value of e and highest value is obtained at $e=1.8$ which is 6.990 m/s that is much higher than 6.474 m/s that was obtained at $e=1.0$. Therefore, for the designing purpose height of rib $e=1.8$ will be considered and corresponding to it value of turbulence kinetic energy and turbulence intensity are highest

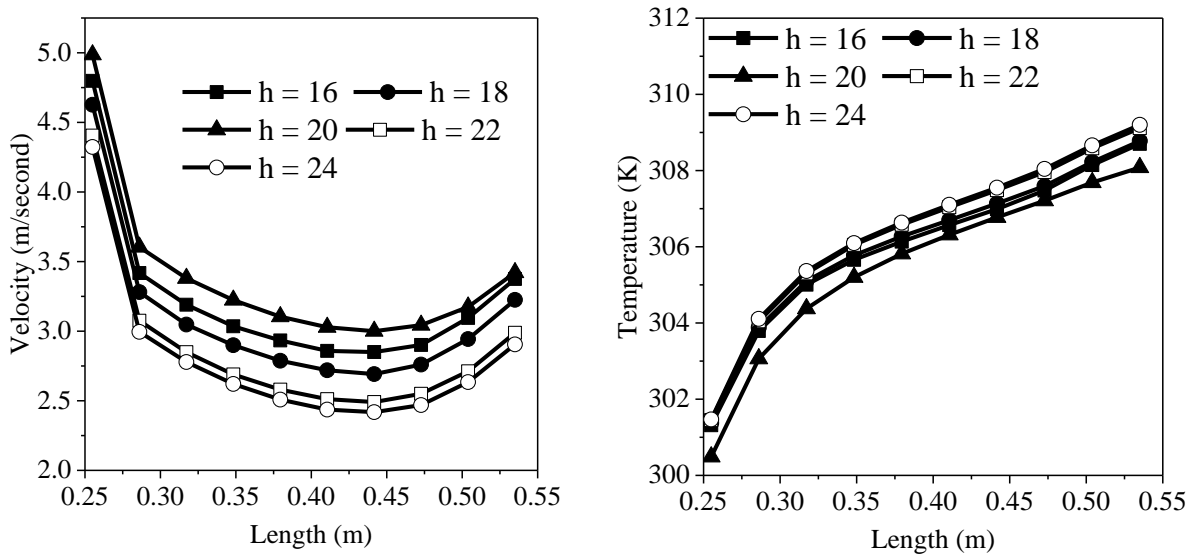
2.894m²/s²and 1.389; respectively. When these two values are high then there will be uniform distribution of temperature throughout the absorber plate. Highest temperature may be obtained for different value as it will be obtained only on the top of plate.

Table 6. Variation of parameters with respect to rib-height (*e*) and depth of duct (*h*) for **Design 3**.

	Velocity (m/s)	Temperature (K)	Turbulence Kinetic Energy (m ² /s ²)	Turbulence Intensity
Rib-height (<i>e</i>)	1.0	6.474	339.2	1.995
	1.2	6.526	342.9	2.124
	1.4	6.737	334.5	2.807
	1.6	6.837	336.9	2.885
	1.8	6.990	333.1	2.894
depth of duct (<i>h</i>)	16	6.850	333.8	3.213
	18	6.790	333.8	2.953
	20	6.737	334.5	2.807
	22	6.696	335	2.704
	24	6.658	335.3	2.608

4.4.2 Effect of depth of duct (*h*)

Next, the effect of depth of duct has been studied with help of **Table 6** here for different values of *h* = 16, 18, 20, 22 and 24 and present numerical results are shown in **Figure 8 (a-d)**. It is evident from the resultant values that the velocity is gradually decreasing on increasing the value of depth of duct which means lowest value of depth of duct needs to be considered, i.e. (*h*=16) for which value of velocity is obtained as 6.850 m/s and highest value of turbulence kinetic energy and turbulence intensity as 3.213m²/s² and 1.461; respectively. Whereas corresponding higher value of temperature as 333.8K. It is found that both designs 2 and 3 have similar. To increase the heat transfer rate the higher value of the rib-height (*e*) and lower value of depth of duct (*h*) is required for good performance of solar air heater.



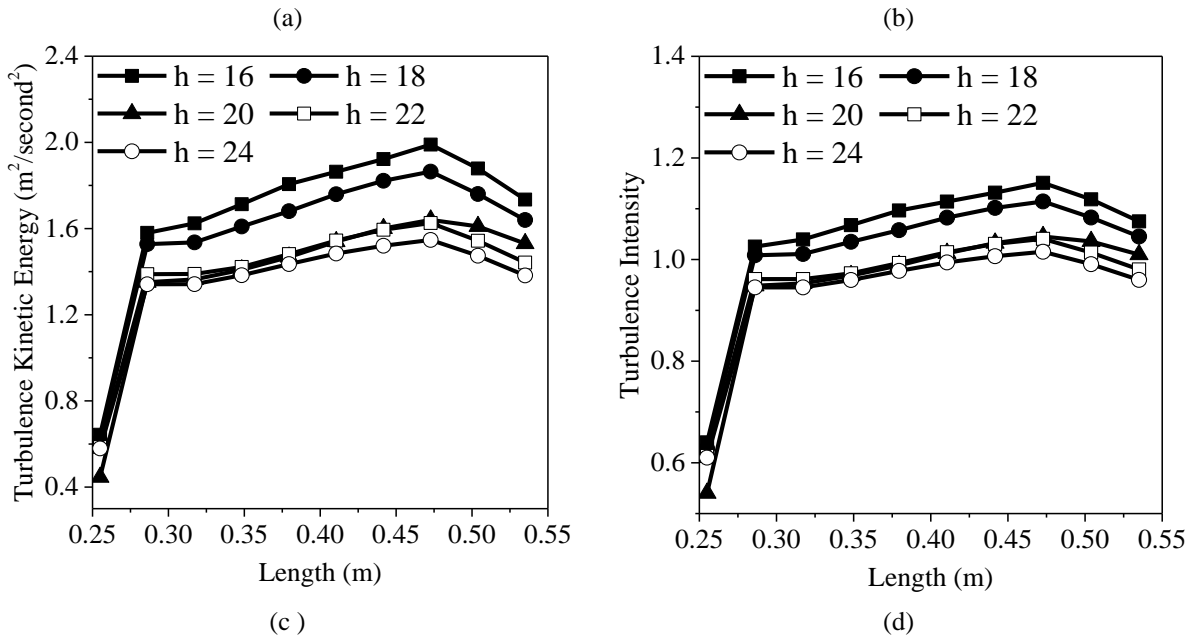
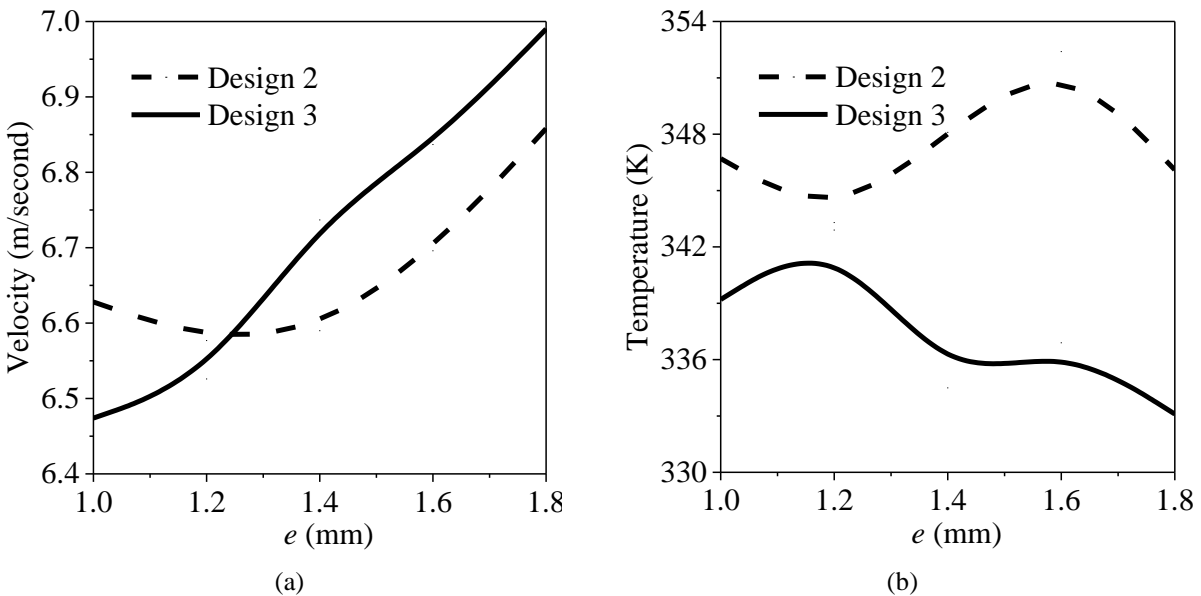


Figure 8. Comparison of different values of h for (a) velocity, (b) temperature, (c) turbulence KE and (d) turbulence intensity for Design 3.

4.5 Comparison in design 2 and 3 by change in rib-height (e)

Next, comparison study is conducted to clearly identify the effects of rib height on design 2 and design 3 as shown in **Figure 9**. It is seen that at starting value of velocity is higher for design 2 but at the end highest value of velocity (velocity $V = 6.990$ m/second) is being observed for design 3 at $e=1.8$; whereas minimum temperature ($T = 333.1$ K) is noticed for design 3 with respect to maximum turbulence kinetic energy and turbulence intensity 2.894 $\text{m}^2/\text{second}^2$ and 1.389 ; respectively. This shows that out of both these new designs, design 3 for value for $e=1.8$ will be selected showing the velocity 7.0 m/s and also the turbulence kinetic energy and turbulence intensity both are higher for design 3 at same rib height ($e = 1.8$).



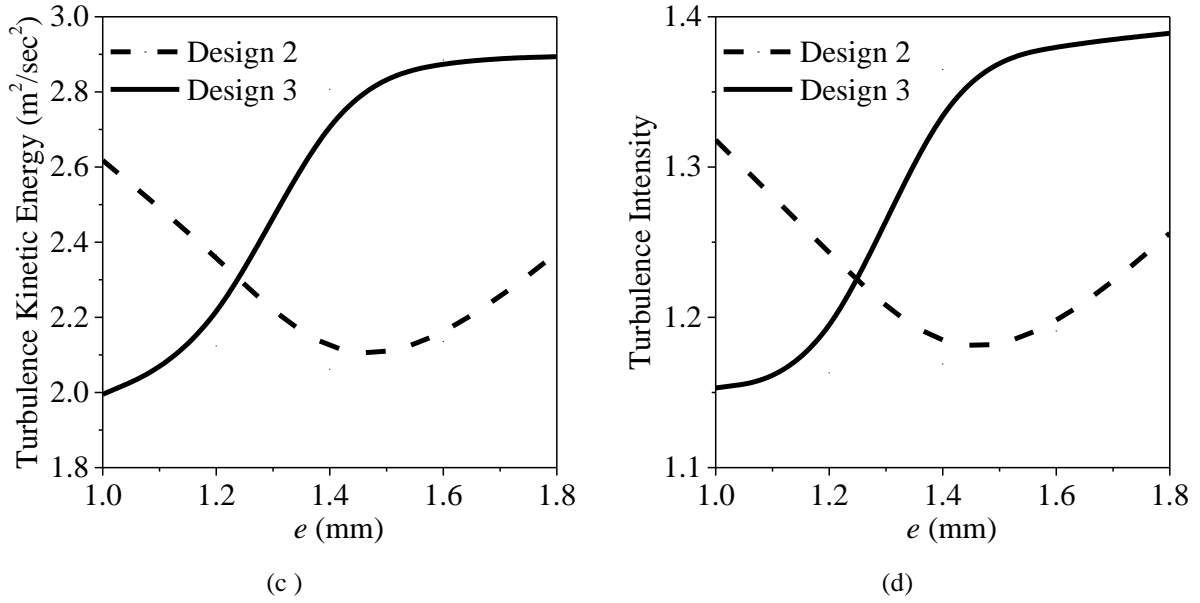
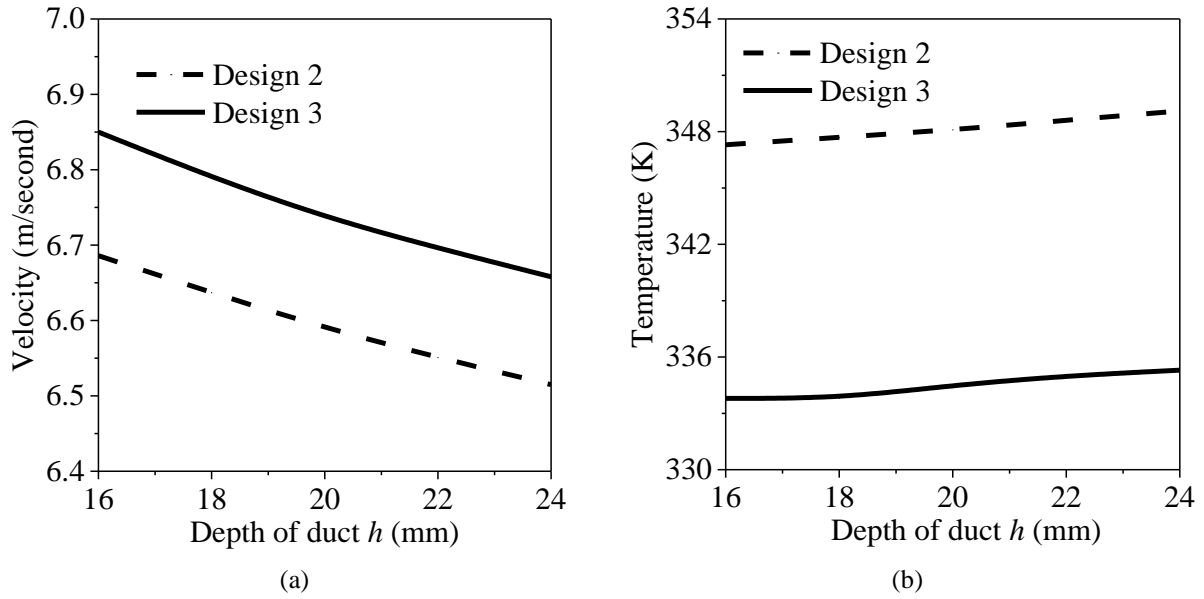


Figure 9. Comparison based graph of Design 2 and Design 3 by variation in e

4.6 Comparison in design 2 and 3 with change in depth of duct (h)



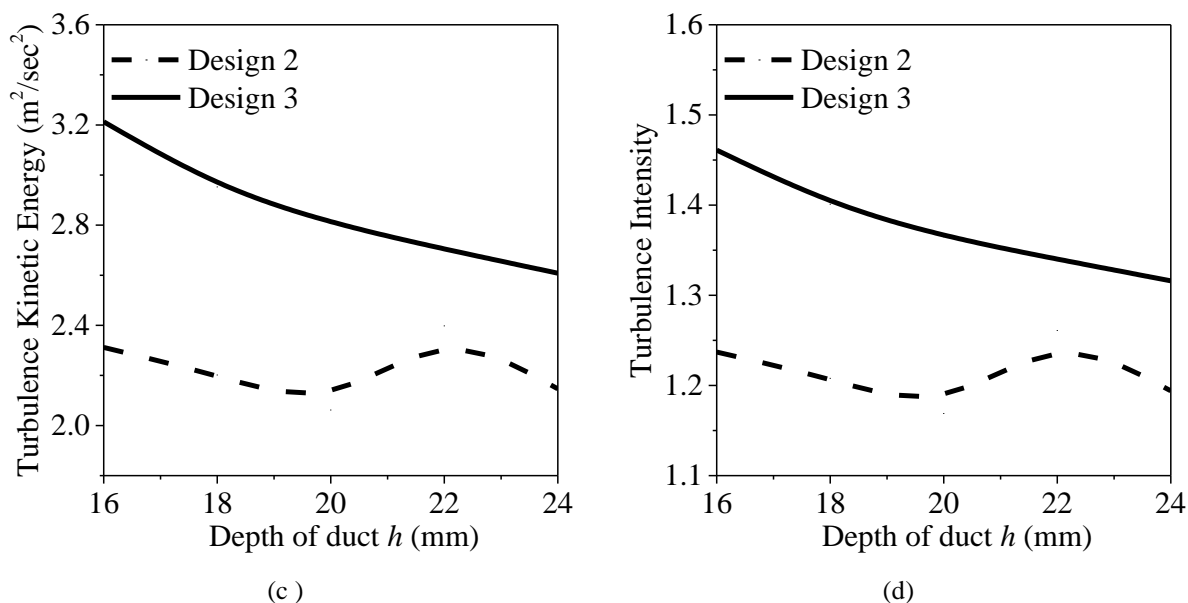


Figure 10. Comparison based graph of Design 2 and Design 3 with change in depth of duct h

Now, investigated the effect of depth of duct ($h = 16, 18, 20, 22$ and 24) and demonstrated the performance of solar air heater in **Figure 10**. It can be clearly seen by graph that at all the points' design 3 have higher velocity than design 2. The highest velocity ($V = 6.850$ m/second) for design 3 is obtained at $h = 16$. Similarly for same value of depth of duct ($h = 16$) the highest value of turbulence kinetic energy (3.213 m²/second²) and turbulence intensity (1.461) is obtained along with high value of temperature ($T = 333.8$ K), therefore this value needs to be considered on the basis of comparison-based study.

5. Conclusion and Future Work

Here, discussed the prospects of design of solar air heater and optimized the performance of solar air heater through computationally fluid dynamic analysis. Authors investigated the effect of velocity, temperature, turbulence kinetic energy and turbulence intensity on design 2 and design 3. For the optimization of solar air heater design, Comparison study has been performed for design 2 and design 3 and studied the effects of various parameters rib-height (e) and depth of duct (h).

From this numerical analysis, it is concluded that the initial velocity of design 2 when rib height $e = 1.0$ the velocity of air in the solar air heater will be $V = 6.628$ m/second that is higher than the design 3 in which velocity will $V = 6.474$ m/second. But when rib-height is increased to $e = 1.8$ then the design 3 have highest velocity $V = 6.990$ m/second among the both the Design 2 and 3. Moreover, design 2 attained more temperature $T = 345$ K than the design 3 which is attains $T = 335$ K. Whereas, the initial turbulence kinetic energy is higher in design 2 2.6 m²/second² for rib height $e = 1.0$ as compare to 1.995 m²/second² for design 3. Maximum turbulence kinetic energy is attained for design 3, which is 2.894 m²/second² when rib-height is $e = 1.8$. Similarly, the initial turbulence energy was higher in design 2 (i.e., 1.3) but at the end, design 3 gained a higher turbulence intensity of 1.4 .

- Different cases were performed by varying depth of duct with keeping rib height constant ($e = 1.4$) in both designs. By comparing all cases with respect to velocity, it is found that velocity will decrease if depth of duct increases.
- Turbulence kinetic energy and turbulence intensity also follows the same trend as velocity with increasing the depth of duct.
- Some cases were performed by varying rib height and keeping depth of duct constant in both designs. As shown in the results, velocity will increase if rib height increased.

- If all cases are considered with all parameters (temperature, velocity, turbulence kinetic energy and turbulence intensity) then the optimized design is design 3 having rib height $e = 1.8$ and depth of duct $h = 16$.

Here, authors optimized the performance of solar air heaters through computational fluid dynamic analysis. Experimental investigation will be carried out in future to optimize the performance of solar air heaters by considering depth of duct and rib height. Moreover, empirical relations will be established for future use.

References

- [1]. S. Haldorai, S. Guruswamy & M. Pradhapraj, "A review on thermal energy storage systems in solar air heater," vol. 43, no.12, pp.6061-6077, International Journal of Energy Research, 2019.
- [2]. M. Sharma, E. Kumari and P.M. Meena, "CFD Analysis on Solar Air Heater to Enhance Heat Transfer- A review," March 2021.
- [3]. A. K Goel, S. N. Singh and B. N. Prasad, "Performance investigation and parametric optimization of eco-friendly sustainable design Solar Air Heater Ribs," vol. 15, no. 12, pp.2645-2656, Wiley Online Library, 2021.
- [4]. H. Huseyin and Y. Demirel, "Exergy-based performance analysis of packed-bed solar air heater," vol. 28, no. 5, pp. 423-432, International Journal of Energy Research, March 2014.
- [5]. P. K. Chaudhary and D. C. Baruah, "Solar air heater for residential space heating," *Energ. Ecol. Environ*, vol.2, no.6, pp.387-403, 2017.
- [6]. S. K. Jain, G. D. Agrawal, and R. Mishra, "Review on thermal performance enhancement of Solar air heater using artificial roughness," *Proc. IEEE Int. Conf. Technol. Adv. Power Energy Explor. Energy Solut. an Intell. Power Grid*, TAP Energy 2017, pp. 1-6, 2018.
- [7]. A. S. Yadav and J. L. Bhagoria, "Modeling and simulation of turbulent flows through a solar air heater having square-sectioned transverse rib roughness on the absorber plate," *Sci. World J.*, vol. 2013, 2013.
- [8]. A. B. Boukadoum and A. Benzaoui, "CFD based analysis of heat transfer enhancement in solar air heater provided with transverse rectangular ribs," *Energy Procedia*, vol.50, pp.761-772, 2014.
- [9]. A. K. Patil, J. S. Saini, and K. Kumar, "A comprehensive review on roughness geometries and investigation techniques used in artificially roughened solar air heaters," *Int. J. Renew. Energy Res.*, vol. 2, no. 1, pp. 1-15, 2012.
- [10]. A. S. Hussien and B. A. Zeru, "Design Optimization and CFD Simulation of Solar Air Heater with Jet Impingement on V-Corrugated Plate," *Int. Res. J. Eng. Technol.*, vol. 7, no. 5, pp. 1805-1813, 2020.
- [11]. R. Ranjan, M. K. Paswan, and N. Prasad, "CFD based Analysis of a Solar Air Heater having Isosceles Right Triangle Rib Roughness on the Absorber Plate," *International Energy Journal*, vol.17, no. 2, pp. 57-74, 2017.
- [12]. J. Rana, A. Silori, R. Maithani, et al., "A CFD thermal Performance analysis of Solar Air Heater with Turbulent Promoters," *J. Basic Appl. Eng. Res.*, vol. 3, no. 12, pp. 1064-1067, 2016.
- [13]. K. Soni and S. Bharti, "CFD Analysis of Solar Air Heater for Enhancement of Heat Transfer," *Int. J. Eng. Sci. Res. Technol.*, vol. 6, no. 6, pp. 430-444, 2017.
- [14]. L. Abhay, V. P. Chandramohan, and V. R. K. Raju, "Numerical analysis on solar air collector provided with artificial square shaped roughness for indirect type solar dryer," *J. Clean. Prod.*, vol. 190, pp. 353-367, 2018.
- [15]. S. W. Ahn & K. P. Son, "An investigation on friction factors and heat transfer coefficients in a rectangular duct with surface roughness," *KSME Int. J.*, vol. 16, no. 4, pp. 549-556, 2002.
- [16]. E. Kumari, & S. Lal, "Nonlinear Bending Analysis of Trapezoidal Panels under Thermo-Mechanical Load," *Forces in Mechanics*, vol.8, 2022.



- [17]. E. Kumari, & D. Saxena, "Buckling analysis of folded structures," *Materials Today: Proceedings*, vol.43, part 2, pp. 1421-1430, 2021.
- [18]. E. Kumari, "Free vibration analysis of rotating laminated composite plate type blades with variable thickness," *Materials Today: Proceedings*, vol. 43, part 2, pp. 1762-1773, 2021.
- [19]. E. Kumari, "Dynamic response of composite panels under thermo-mechanical loading," *Journal of Mechanical Science and Technology*, vol.36, no.8, pp. 3781-3790, 2022.

